Characterization of the Transition-State Structure of the Reaction of Kanamycin Nucleotidyltransferase by Heavy-Atom Kinetic Isotope Effects†

Barbara Gerratana, Perry A. Frey, and W. W. Cleland*

Institute for Enzyme Research, Department of Biochemistry, College of Agricultural Life Sciences, 1710 University Avenue, University of Wisconsin−Madison, Madison, Wisconsin 53705

Received November 6, 2000; Revised Manuscript Received January 17, 2001

ABSTRACT: The transition-state structure for the reaction catalyzed by kanamycin nucleotidyltransferase has been determined from kinetic isotope effects. The primary ^{18}O isotope effects at pH 5.7 (close to the optimum pH) and at pH 7.7 (away from the optimum pH) are respectively 1.016 ± 0.003 and 1.014 ± 0.002. Secondary ^{18}O isotope effects of 1.0033 ± 0.0004 and 1.0024 ± 0.0002 for both nonbridge oxygen atoms were measured respectively at pH 5.7 and 7.7. These isotope effects are consistent with a concerted reaction with a slightly associative transition-state structure.

Aminoglycoside antibiotics have been extensively used to treat bacterial infections. In recent years, a growing number of bacterial strains resistant to the aminoglycoside antibiotics have been isolated (*1*). The main biochemical mechanism of the bacterial antibiotic resistance is the enzymatic modification of the aminoglycoside such as the nucleotidylation of a hydroxyl group of the aminoglycoside catalyzed by the *O*-nucleotidyltransferases (ANT) (*2*). A member of this class is kanamycin nucleotidyltransferase[1] (ANT-4′,4″)-I from *Staphylococcus aureus* which catalyzes the transfer of AMP moiety from ATP to the 4′ hydroxyl group of kanamycin A (Scheme 1) (*3*). KNTase is an homodimer as shown by the crystal structure of the KNTase thermostable mutant D80Y (TK1) solved with KanA and AMPCPP (*4*). KNTase has a broad range of substrate specificity for both the aminoglycoside (*5*, *6*) and the nucleotide (ATP, GTP, dTTP, UTP, and *m*NBTP) (*3*, *6*). The reaction of KNTase with KanA and ATP follows an ordered Bi−Bi mechanism (*6*) with the chemistry step not rate limiting. The reaction of KNTase with the substrate analogue *m*NBTP is 2 orders of magnitude slower than with ATP but it has the same regiospecificity (*3*). In this report, we established that the chemistry is rate limiting in the reaction of KNTase with *m*NBTP.

Enzymatic and nonenzymatic substitution reactions at phosphate esters have been shown to employ one of two stepwise mechanisms or a concerted mechanism. A fully dissociative mechanism ($D_N + A_N$) is characterized by a metaphosphate intermediate, while a pentacoordinate phosphorane intermediate, in which the sum of the axial bond orders is equal to two, describes a stepwise associative mechanism ($A_N + D_N$) (*7*). In the concerted mechanism of phosphoryl transfer reactions, the character of the transition state ranges from associative with the sum of the axial bonds between one and two, to S_N2 with the sum of the axial bonds equal to 1, to dissociative with the sum of the axial bonds less than one. An associative transition state resembles a phosphorane, thus it is referred to as a phophorane-like transition state. A dissociative transition state resembles metaphosphate and is referred to as a metaphosphate-like transition state (*7*).

Substitution reactions at tetrahedral phosphate esters are very common in biological systems. The mechanism and the structure of the transition state of enzymatic and nonenzymatic reactions have been the focus of a lively debate (*8*, *9*). The hydrolysis of monoesters is characterized by a dissociative transition state in both enzymatic (*7*, *10*) and nonenzymatic reactions (*11*, *12*). Phosphotriester cleavage is a concerted reaction with an associative transition state in both chemical and enzymatic reactions (*12*, *13*). A phosphorane intermediate is characteristic for reaction of cyclic esters and when geometry demands pseudorotation in order to position the leaving group in axial position (*14*, *15*). Kinetic isotope effect studies of enzymatic reactions (*7*) and of alkaline hydrolysis of phosphodiesters (*7*, *14*) show that these reactions are concerted with slightly associative transition states. Under acidic conditions cleavage of phosphodiesters proceeds through a phosphorane intermediate (*14*); a concerted mechanism is characteristic of a phosphodiester with a good leaving group (*7*). Thus, in general transition states become more associative with an increased degree of esterification.

Heavy-atom kinetic isotope effects have been extensively used to study transition-state structures of enzymatic and nonenzymatic phosphoryl transfer reactions (*7*, *10*). The size of the primary isotope effect, $^{18}(V/K)_{bridge}$, is an indication of the degree of bond breaking measured at the leaving group oxygen atom in the transition state and to what extent the chemistry is rate limiting. The partial loss or increase of bond

†This work was supported by NIH Grant GM18938 to W.W.C.

* To whom correspondence should be addressed. Phone: (608) 262-1373. Fax: (608) 265-2904. E-mail: cleland@biochem.wisc.edu.

[1] Abbreviations: KNTase, kanamycin nucleotidyltransferase; TK1, D80Y KNTase thermostable variant; KanA, kanamycin A; KanA-AMP, 4′-(adenosine-5′-phosphoryl)-kanamycin A; KanA-*m*NBMP, 4′-(*m*-nitrobenzyl phosphoryl)-kanamycin A; *m*NBTP, *m*-nitrobenzyl triphosphate; AMPCPP, adenosine 5′-α,*β*-methylenetriphosphate; TEAB, triethylammonium bicarbonate; MALDI-TOF, matrix-assisted laser desorption time-of-flight mass spectrometry.

10.1021/bi002557x CCC: $20.00
Published on Web 02/07/2001

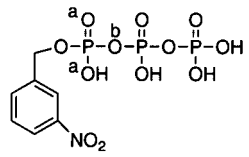

FIGURE 1: *m*-Nitrobenzyl triphosphate showing the positions of the isotope effect measured in the reaction of kanamycin nucleotidyltransferase with KanA. (a) $^{18}(V/K)_{nonbridge}$ measured at the nonbridge oxygen atoms. (b) $^{18}(V/K)_{bridge}$ measured at the bridge oxygen atom.

order between the nonbridge oxygen atoms and the phosphorus atom in the transition state is revealed by the secondary kinetic isotope effect, $^{18}(V/K)_{nonbridge}$. We report the kinetic isotope effects for the reaction of kanamycin nucleotidyltransferase with the remote-labeled *m*NBTP (Figure 1), a slow substrate analogue (*3*).

EXPERIMENTAL PROCEDURES

Materials and Methods. All the buffers and chemicals were from Aldrich. KanA, all coupling enzymes, and all resins were from Sigma. $H_2{}^{18}O$, $^{14}NH_4{}^{14}NO_3$, and $^{15}NH_4{}^{15}NO_3$ were from Isotec. $^{18}O_4$-dibasic sodium phosphate from Miles-Yeda Inc. was a generous gift from Prof. H. A. Lardy, Institute for Enzyme Research, University of Wisconsin-Madison. Plasmid pALT/TK1 was a generous gift from Prof. H. M. Holden, Department of Biochemistry, University of Wisconsin—Madison. Vyadac 302IC4.6 HPLC column was from Vyadac. A Microsorb-MV C18 HPLC column was from Varian Analytical Instruments. The identity of the synthesized compounds was checked by NMR spectrometry, and the compounds were pure within the limitation of detection of the NMR spectrometer. ^{1}H and ^{31}P spectra were recorded on a Bruker 200 MHz instrument, operating at 81 MHz for ^{31}P experiments. Phosphorus spectra were referenced to an external standard of 85% phosphoric acid. MALDI-TOF mass spectra were collected in the negative mode on a Bruker Reflex II TOF-MS equipped with a N_2 laser. The matrix used for all experiments was α-cyano-4-hydroxycinnamic acid. Samples were prepared in the NH_4^+ form using cation-exchange resin.

Purification and Activity Assay of KNTase. The KNTase thermostable mutant, D80Y (TK1), was purified following the procedure described in Gerratana et al. (*3*). The enzyme purity was determined to be greater than 95% by SDS−PAGE gel. The activity of kanamycin nucleotidyltransferase was assayed using a coupled enzyme assay that detects pyrophosphate by the action of UDP-glucose pyrophosphorylase, phosphoglucomutase and glucose-6-phosphate dehydrogenase (*3*).

Synthesis of [^{14}N]- and [^{15}N]-m-nitrobenzyl bromide. A solution of $^{14}NH_4{}^{14}NO_3$ or $^{15}NH_4{}^{15}NO_3$ (47 mmol) in 25 mL of concentrated sulfuric acid was added slowly to a solution of benzaldehyde (47 mmol) in 25 mL of concentrated sulfuric acid at 0 °C under nitrogen. The mixture was stirred for 30 min, and *m*-nitrobenzaldehyde (33.1 mmol) was precipitated by adding ice-cold water. Dry *m*-nitrobenzaldehyde was dissolved in 100 mL of anhydrous methanol in ice under nitrogen. To the *m*-nitrobenzaldehyde solution $NaBH_4$ (66 mmol) was added slowly, and the solution was stirred for an additional 20 min at the end of which 20 mL of distilled H_2O were added. The solution was titrated to pH 7.0 with 6 N HCl. Removal of methanol by rotary evaporation was followed by three extractions with diethyl ether. The combined ether layers containing *m*-nitrobenzyl alcohol were dried over $MgSO_4$ and concentrated. Dry [^{15}N]- or [^{14}N]-*m*-nitrobenzyl alcohol (20 mmol) was brominated in anhydrous toluene with phosphorus tribromide (25 mmol) according to the procedure of Kornblum and Iffland (*16*). [^{14}N]- or [^{15}N]-*m*-nitrobenzyl bromide was crystallized from cold petroleum ether and 16 mmol of the crystalline product were obtained (*16*).

Synthesis of mNBTP and [^{14}N]-mNBTP. Natural abundance *m*NBTP was synthesized as previously described (*3*). The same procedure was used to prepare [^{14}N]-*m*NBTP with the exception that [^{14}N]-*m*-nitrobenzyl bromide was used as starting material.

Scheme 1

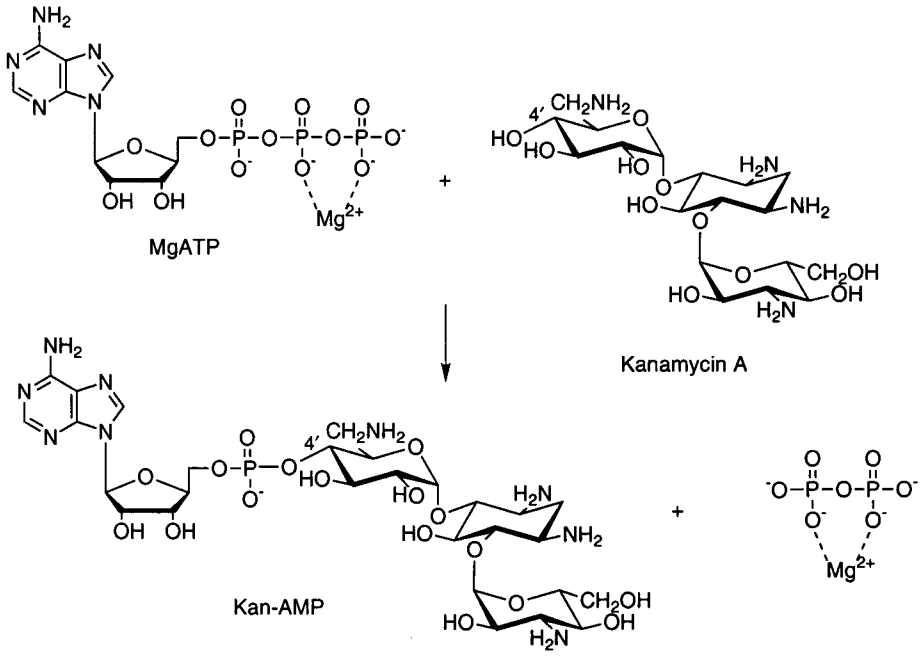

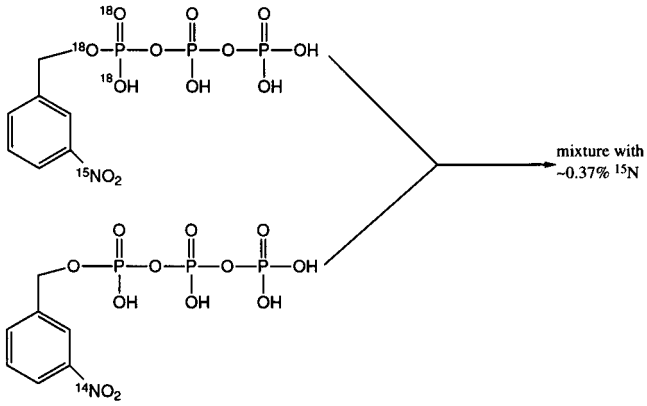

FIGURE 2: Substrate mixture used to measure the secondary kinetic isotope effects. [^{14}N]*m*NBTP and [α-$^{18}O_3$,^{15}N]-*m*NBTP are mixed together to reconstitute the natural abundance at the remote position.

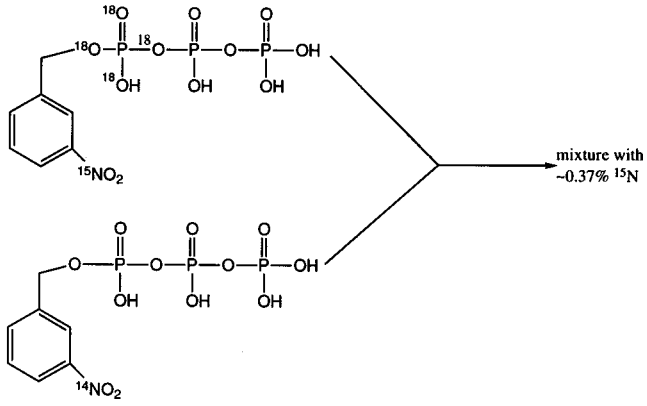

FIGURE 3: Substrate mixture used to measure the combined primary and secondary kinetic isotope effects. [^{14}N]*m*NBTP and [α-$^{18}O_3$,αβ-^{18}O,^{15}N]-*m*NBTP are mixed together to reconstitute the natural abundance at the remote position.

Synthesis of [α-$^{18}O_3$,αβ-^{18}O,^{15}N]-mNBTP. [γ-$^{18}O_3$,βγ-^{18}O]-ATP was prepared from the tributylammonium salts of ADP and of $P^{18}O_4$ by the method of Webb (*17*). [α-$^{18}O_3$,αβ-^{18}O,^{15}N]-*m*NBTP was synthesized following the procedure already reported (*3*) using [γ-$^{18}O_3$,βγ-^{18}O]-ATP and [^{15}N]-*m*-nitrobenzyl bromide as starting material. The MALDI spectrum showed [α-$^{18}O_3$,αβ-^{18}O,^{15}N]-*m*NBTP to have 75% [$^{18}O_4$], 17% [$^{18}O_3$], and 8% [$^{18}O_0$] material.

Synthesis of [α-$^{18}O_3$,^{15}N]-mNBTP. [$^{18}O_3$]Phosphoenolpyruvate was synthesized in $H_2{}^{18}O$ (93% ^{18}O) by acid-catalyzed exchange (*18*). [γ-$^{18}O_3$]ATP was prepared from ADP and [$^{18}O_3$]phosphoenolpyruvate with pyruvate kinase at pH 7.0 and it was purified as for [γ-$^{18}O_3$,βγ-^{18}O]ATP. [α-$^{18}O_3$,^{15}N]*m*NBTP was synthesized following the procedure already reported (*3*) using [γ-$^{18}O_3$]ATP and [^{15}N]-*m*-nitrobenzyl bromide as starting material. The MALDI spectrum showed [α-$^{18}O_3$,^{15}N]*m*NBTP to have 44% [$^{18}O_3$], 37% [$^{18}O_2$], 9% [$^{18}O_1$], and 10% [$^{18}O_0$] material.

Kinetic Isotope Effect Determinations. The remote label method was used to measure the kinetic isotope effects (*19*). Substrate labeled at both the position of interest and the remote label position was added to substrate depleted in the heavy atom at the remote label position to reconstitute the natural abundance at the remote position. The substrate labeled mixture used to measure the secondary isotope effects was obtained by mixing [α-$^{18}O_3$,^{15}N]-*m*NBTP with [^{14}N]-*m*NBTP (Figure 2). The combined bridge and nonbridge kinetic isotope effects were measured with [^{14}N]*m*NBTP and [α-$^{18}O_3$,αβ-^{18}O,^{15}N]-*m*NBTP (Figure 3). In the KNTase reaction the nitrogen of the nitro group in the substrate *m*NBTP is the remote label. Prior to use in the KNTase reaction, the substrate labeled mixture was purified on a DEAE Sephadex A25 (HCO_3^- form) column (2.5 cm × 20 cm) with a 2 L linear gradient of 0.3 to 0.9 M TEAB, pH 7.6. After removal of TEAB at 25 °C by repeated washes with 50% methanol on a rotary evaporator under vacuum, the sodium salt was obtained by eluting with distilled H_2O through a column of SP Sephadex C25 (Na^+ form). A 1.7 mM solution of the appropriate labeled mixture of *m*NBTP (34 μmol) was prepared with 30 μmol of KanA, 1 mM DTT, 10 mM $MgCl_2$, and 5 unit/mL of inorganic pyrophosphatase in 20 mL of 50 mM acetate buffer for the reactions at pH 5.7 and 50 mM Tris buffer for reactions at pH 7.7. For the reactions at pH 5.7, 40−50 mg of KNTase was used, while for reactions at pH 7.7, 10 mg of KNTase was added. The reaction was followed by HPLC using a Vyadac 302IC4.6 column (4.6 mm × 250 mm) with buffer A from 0 to 3 min. From 3 to 18 min, a gradient was applied from buffer A to buffer B. Buffer A was 0.05 M K_2HPO_4/KH_2PO_4 (molar ratio 1:1) adjusted to pH 2.85 with acetic acid. Buffer B was 0.30 M K_2HPO_4/KH_2PO_4 (molar ratio 1:1) adjusted to pH 2.93 with acetic acid. Detection was accomplished by absorption at 270 nm. At 2 mL/min, KanA-*m*NBMP elutes at 1.6 min and *m*NBTP at 16 min. Reactions were stopped by removal of the enzyme by filtration with a PM10 Amicon filter at 4 °C, and the fraction of product formed was determined by analytical HPLC as described above. The filtered solution was loaded on a DEAE Sephadex A25 (HCO_3^- form) column (2.5 cm × 20 cm). After eluting Kan-*m*NBMP with distilled H_2O, the residual *m*NBTP was eluted with a 1.5 L linear gradient of 0−0.9 M TEAB, pH 7.6. The fractions containing product Kan-*m*NBMP were collected and titrated to pH 3.0 with 1 N HCl. The solution was washed three times with freshly distilled diethyl ether and then concentrated to ∼20 mL. This solution was made 1 N in HCl, and Kan-*m*NBMP was hydrolyzed at 95 °C for 48−72 h. The hydrolysis was followed by HPLC using a Microsorb-MV C18 HPLC column (5 μm, 4.6 mm × 250 mm) equilibrated with 6 mM NaH_2PO_4, pH 6.8, in 27% methanol. Detection was by absorption at 270 nm. Kan-*m*NBMP emerged as a broad peak between 8 and 10 min, *m*NBMP at 4 min and *m*-nitrobenzyl alcohol at 18.2 min. When the hydrolysis was completed, *m*-nitrobenzyl alcohol was extracted three times with distilled diethyl ether. The ether layers were combined and ether was removed by rotary evaporation. The residue was then diluted in ∼20 mL of distilled H_2O and titrated to pH 11 with 2 N KOH. *m*-Nitrobenzyl alcohol was reextracted three times with diethyl ether. The combined ether layers were dried over anhydrous $MgSO_4$, concentrated by rotary evaporation and sublimed at 95 °C for 20 min (*20*).

After removal of TEAB at 25 °C by repeated washes under vacuum with 50% methanol on a rotary evaporator, the solution containing the residual substrate was loaded on a column of SP Sephadex C25 (Na^+ form). The sodium salt of *m*NBTP was eluted with distilled H_2O and the combined fractions were concentrated to ∼20 mL and made 1 N in HCl. *m*NBTP was hydrolyzed to *m*-nitrobenzyl alcohol at 95 °C for 5−6 days. The hydrolysis was followed by HPLC with a Vyadac 302IC4.6 column (4.6 mm × 250 mm) as described above. *m*-Nitrobenzyl diphosphate and monophos-

Table 1: Kinetic Isotope Effects[a] for the Reaction of Kanamycin Nucleotidyltransferase with *m*NBTP and KanA at 25 °C

pH	$^{15}(V/K)$	$^{18}(V/K)_{nonbridge}$[b]	$^{18}(V/K)_{(nonbridge)(bridge)}$	$^{18}(V/K)_{bridge}$[c]
5.70	1.0011 ± 0.0009 (6)	1.0033 ± 0.0004 (5)	1.019 ± 0.003 (5)	1.016 ± 0.003
7.70	nd	1.0024 ± 0.0002 (6)	1.016 ± 0.002 (5)	1.014 ± 0.002

[a] Uncertainties reported are the standard errors. The number of determinations are in parentheses. [b] Kinetic isotope effect for ^{18}O in both nonbridge oxygen atoms. [c] Isotope effects corrected from the secondary isotope effects using the equation: $^{18}(V/K)_{bridge} = {}^{18}(V/K)_{(nonbridge)(bridge)}/{}^{18}(V/K)_{nonbridge}$.

phate emerge, respectively, at 14 and 11 min, *m*-nitrobenzyl alcohol at 3 min, and *m*NBTP at 16 min. When hydrolysis was completed, the solution containing *m*-nitrobenzyl alcohol was extracted and treated as described above. The initial isotopic composition in the substrate mixture used was determined by hydrolyzing *m*NBTP to *m*-nitrobenzyl alcohol as described above for the residual substrate. The isotopic composition of each sample was analyzed with an elemental analyzer (Carlo Erba-NA 1500 Series 2) coupled with an Europa Tracermass 20−20 isotope ratio mass spectrometer.

Data Analysis. The isotope effects were calculated from the following equations:

$$^{18}(V/K)_{obs} = \log(1 - f)/\log[1 - f(R_p/R_o)] \quad (1)$$

$$^{18}(V/K)_{obs} = \log(1 - f)/\log[(1 - f)(R_s/R_o)] \quad (2)$$

where f is the fraction of the KNTase reaction, R_o is the isotopic ratio in the starting mixture of labeled *m*NBTP, R_s is the isotopic ratio in the residual substrate, and R_p is the isotopic ratio in Kan-*m*NBMP product at partial reaction. The $^{15}(V/K)$ values were calculated from eqs 1 and 2. The $^{18}(V/K)_{obs}$ values calculated from eqs 1 and 2 were corrected for incomplete isotopic incorporation in the starting material using the remote label equations (*13*).

RESULTS

In Table 1 the kinetic isotope effects are reported with their standard errors (see Supporting Information for a complete list of all single isotope effects measured). Each isotope effect listed is the average of multiple experiments performed under the given conditions. The isotope effects determined from the product using eq 1 were in agreement, within experiemental error, with those determined from the residual substrate using eq 2; thus they were averaged together. The isotope effects listed are on *V*/*K* since they were measured by the method of internal competition. The optimum pH for the KNTase reaction with *m*NBTP is 5.0 (*3*). By the time 20−50% of the substrate was converted to product at pH 5.0 the enzyme had become unstable and had lost activity, thus the reactions were run at pH 5.7, close to the pH optimum, to minimize the amount of KNTase necessary to have partial conversion. The kinetic isotope effect experiments were run also at pH 7.7, far from the pH optimum, where the chemical step is more likely to be rate limiting.

The kinetic isotope effects measured using natural abundance material at the remote label position was unity within experimental error, which is expected because no change in bond order to the nitrogen atom of the nitro group of *m*NBTP should occur during the reaction. Thus, the $^{15}(V/K)$ effect did not contribute to the ^{18}O effects listed in Table 1 which were corrected only for the isotopic incorporation (*13*). The kinetic isotope effect measured with [α-$^{18}O_3$,αβ-^{18}O,^{15}N]- and [^{14}N]*m*NBTP mixture (Figure 3) has contributions from both the primary effect and the secondary effect. This effect is divided by the secondary isotope effect already measured in order to obtain the primary isotope effect reported. Both remote labeled substrates contained ^{18}O in the benzyl alcohol−α-phosphate bond. Since this oxygen does not change its bonding during the reaction, we have assumed that the ^{18}O substitution at this position does not cause an isotope effect.

DISCUSSION

The mechanisms and transition-state structures of chemical reactions have been successfully investigated through kinetic isotope effect studies. Kinetic isotope effects reflect changes in bond order between the ground state and the transition state of the rate-limiting step. The interpretation of kinetic isotope effects measured on enzymatic reactions is complicated by the existence of other steps such as substrate binding, conformational changes and product release, which are often partially or totally rate limiting. The isotope effects measured by the internal competition method are effects on *V*/*K*; thus, they take in account any steps up to and including the first irreversible step. In the reaction of alkaline phosphatase with *p*-nitrophenyl phosphate the isotope effects measured were close to unity indicating that a nonchemical step prior to the first irreversible step was rate limiting (*21*). Thus, the full intrinsic isotope effect on the chemical step was suppressed by a commitment factor. To facilitate the observation of the intrinsic isotope effect in the reaction of kanamycin nucleotidyltransferase the substrate analogue *m*NBTP was used which has a k_{cat}/K_m 2 orders of magnitude lower than the k_{cat}/K_m of the KNTase reaction with ATP (*3*). Nonproductive binding, due to the lack of specific interactions with the ribose ring (*4*), may cause the smaller value of k_{cat}/K_m for *m*NBTP reaction. $^{18}(V/K)$ isotope effects are not altered by nonproductive binding. *m*NBTP was also chosen because (1) it retains the triphosphate moiety which is responsible for the majority of the nucleotide-protein interactions as shown by the crystal structure (*4*), (2) the nitrogen in the nitro group of *m*NBTP is an ideal position to function as remote label, and (3) the nucleophile and the leaving group are the same in both reactions of KNTase with ATP or with *m*NBTP.

One way to determine the absence of a commitment in the kinetic isotope effects is to measure the isotope effects at the optimum pH and at a pH well away from the optimum where incorrect protonation of the catalytic groups decreases the rate of the chemical step and consequently the commitment factor. The constant primary isotope effects measured for the KNTase reaction with KanA and *m*NBTP (Table 1) near the pH optimum (pH 5.7) and away from the pH optimum (pH 7.7) (*3*) are evidence of the absence of significant commitment factors in this reaction. Thus, the kinetic isotope effects measured are likely to be the intrinsic

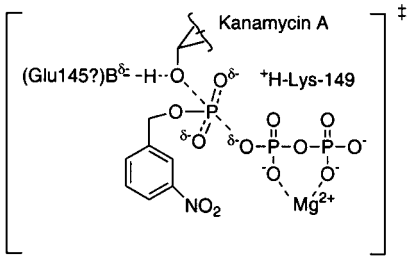

FIGURE 4: Proposed transition-state structure for the kanamycin nucleotidyltransferase catalyzed reaction.

effects for the chemical step and they reflect the structure of the transition state of the chemical step.

The primary isotope effect of 1.6% reflects a considerable loss of bond order between the phosphorus atom and the bridge oxygen in the transition state. The size of the primary effect is consistent with a concerted mechanism or with a stepwise mechanism with a phosphorane intermediate in which the rate-limiting step is the breakdown of the phosphorane intermediate. To distinguish between these two mechanisms the secondary isotope effects have been measured. If a monoanionic phosphorane intermediate were present, a secondary isotope effect of unity would be expected and would be also consistent with an S_N2 mechanism, as in the pH independent cleavage reaction of uridine 3′-*m*-nitrobenzyl phosphate in which an intrinsic primary isotope effect of 1.8% and a secondary isotope effect of unity were measured (*14*). The existence of a dianionic phosphorane is unlikely due to instability of such an intermediate (*22*). An inverse secondary isotope effect would validate a concerted mechanism with partial or full protonation of the nonbridge oxygen of the phosphorane-like transition state as in the phosphodiesterase reaction with *p-tert*-butylphenyl *p*-nitrophenyl phosphate and with 3,3-dimethyl *p*-nitrophenyl phosphate (*23*). However a slightly normal secondary kinetic isotope effect (0.3% at pH 5.7 and 0.2% at pH 7.7) was measured for the KNTase reaction with *m*NBTP. This normal effect reflects loss of bond order at the nonbridge oxygens in the transition state with respect to the ground state. Thus, the primary and secondary kinetic isotope effects are consistent with a concerted mechanism with a slightly associative transition-state structure as shown in Figure 4. The transition-state structure determined for the reaction of KNTase with *m*NBTP can be used as a model for the transition-state structure of the reaction of KNTase with ATP, since in both reactions the nucleophile and the leaving groups are the same.

From the crystal structure of kanamycin nucleotidyltransferase, Glu-145 has been proposed to act as the general base and Lys-149 was shown to be close to the α-nonbridge oxygens (*4*), which may contribute in stabilizing the increased negative charge on the nonbridge oxygens in the transition state. This transition state structure resembles that of the reaction of Ribonuclease A with uridine 3′-*m*-nitrobenzyl phosphate in which a primary isotope effect of 1.6% and a secondary isotope effect of 0.5% were measured (*20*).

The relevance of this study is the determination for the first time of the transition-state structure of a nucleotidyltransferase reaction. In the larger context of the study of the chemical mechanism of phosphoryl transfer in enzyme catalyzed reactions, it also provides the third example of the transition-state structure for enzymatic phosphodiester reaction (*7*). The general trend of increased associative character of the transition-state structure in reaction with phosphoester with higher degree of esterification is also confirmed. In addition, the new information provided on kanamycin nucleotidyltransferase by this report and the the preceding paper in this issue (*3*) will be useful in designing drugs able to prevent its deleterious reaction on aminoglycoside antibiotics.

ACKNOWLEDGMENT

We thank Armand R. Krueger of the Horticulture Department at the University of Wisconsin—Madison for use of the Europa Tracermass 20-20 isotope ratio mass spectrometer.

SUPPORTING INFORMATION AVAILABLE

All the isotope effects measured and the *f* values for all the experiments run at pH 5.70 and pH 7.70. This material is available free of charge via the Internet at http://pubs.acs.org.

REFERENCES

1. Davies, J. E. (1991) in *Antibiotics in Laboratory Medicine* (Lorian, V., Ed.) pp 691−713, Williams & Wilkins, Baltimore, MD.
2. Shaw, K. J., Ralter, P. N., Hare, R. S., and Miller, G. H. (1993) *Microbiol. Rev. 57*, 138−163.
3. Gerratana, B., Cleland, W. W., and Reinhardt, L. A. (2001) *Biochemistry 40*, 2964−2971.
4. Pedersen, L. C., Benning, M. M., and Holden, H. M. (1995) *Biochemistry 34*, 13305−13311.
5. LeGoffic, F., Baca, B., Soussy, C. J., Dublanchet, A., and Duval, J. (1976) *Ann. Microbiol. 127A*, 391−399.
6. Chen-Goodspeed, M., Vanhooke, J. L., Holden, H. M., and Raushel, F. M. (1999) *Bioorg. Chem. 27*, 395−408.
7. Cleland, W. W. (1999) in *Enzymatic Mechanisms* (Frey, P. A., and Northrop, D. B., Eds.) pp 8−19, IOS press, Washington DC.
8. Hasset, A., Blätter, W., and Knowles, J. R. (1982) *Biochemistry 21*, 6335−6340.
9. Herschlag, D., and Jencks, W. P (1990) *Biochemistry 29*, 5172−5179.
10. Cleland, W. W., and Hengge, A. C. (1995) *FASEB J. 9*, 1585−1594.
11. Herschlag, D., and Jencks, W. P (1989) *J. Am. Chem. Soc. 111*, 7579−7586.
12. Benkovic, S. J., and Schray, K. J. (1978) in *Transition States of Biochemical Processes* (Gandour, R. D., and Schowen, R. L., Eds.) pp 493−521, Plenum Press, New York.
13. Caldwell, S. R., Raushel, F. M., Weiss, P. M., and Cleland, W. W. (1991) *Biochemistry 30*, 7444−7450.
14. Gerratana, B., Sowa, G. A., and Cleland, W. W. (2000) *J. Am. Chem. Soc. 122*, 12615−12621.
15. Haake, P. C., and Westheimer, F. H. (1961) *J. Am. Chem. Soc. 83*, 1102−1109
16. Kornblum, N., and Iffland, D. C. (1949) *J. Am. Chem. Soc. 71*, 2137−2143.
17. Webb, M. R. (1980) *Biochemistry 19*, 4744−4748.
18. O′Neal, C. C., Bild, G. S., and Smith, L. T. (1983) *Biochemistry 22*, 611−617.
19. O'Leary, M. H., and Marlier, J. F. (1979) *J. Am. Chem. Soc. 101*, 3300−3306.
20. Sowa, G. A., Hengge, A. C., and Cleland, W. W. (1997) *J. Am. Chem. Soc. 119*, 2319−2320.

21. Hengge, A. C., Edens, W. A., and Elsing, H. (1994) *J. Am. Chem. Soc. 116*, 5045−5049.
22. Lim, C., and Karplus, M. (1990) *J. Am. Chem. Soc. 112*, 5872−5873.
23. Hengge, A. C., Tobin, A. E., and Cleland, W. W. (1995) *J. Am. Chem. Soc. 117*, 5919−5926.

BI002557X